

Numerical and Experimental Study of Drag and Vortex Shedding across Smooth Circular Cylinder with Attached Rigid Bilateral Splitter Plates in Sub-Critical Regime for Landing Gear

M. I. Khan¹, S. A. Masood², S. Zahid³

^{1,2} Department. of Mechanical Engineering, Faculty of Engineering & Technology, International Islamic University, H-10, Islamabad, Pakistan,

³ Mechanical Engineering Department, University of Engineering and Technology Taxila, Pakistan,

¹ Muhammad.ishfaq@iiu.edu.pk

Abstract- Circular cylinder with attached rigid bilateral plates is the most recent approach to suppress vortex shedding passively, especially in applications like landing gear of an aero plane. In this research, attached rigid bilateral splitter plates each having length equal to diameter of circular cylinder have been numerically and experimentally explored from Reynolds Number 4.78×10^4 to 1.35×10^5 in sub-critical regime. The flow has been simulated by employing URAN SST $k-\omega$ model and the results are benchmarked against experimental values of Co-efficient of Drag (Cd). Vortex shedding suppression has been quantified in terms of Strouhal Number (St). The results of this research in terms of Cd and St for applications like landing gear of aero plane are lower than that of bare circular cylinder.

Keywords- : Drag, Reynolds Number, Circular Cylinder, Splitter Plate, Sub-critical Regime

I. INTRODUCTION

In engineering applications like industrial chimneys, bridge columns, supporting cables and strut of landing gear of an aero plane etc. fluid flows across a circular cylinder. Phenomenon of vortex shedding is observed at high Reynolds Number (Re) in these applications. [1-3] This vortex shedding induces vibration into the structure leading to uncomfortable user experience and material loss by structural failure by fatigue and/or resonance in all applications. However, in case of applications like aero plane, this vortex shedding generates higher drag resulting in greater fuel consumptions. Researchers are putting lot of efforts to figure out ways to reduce vortex induced vibrations (VIV) and drag in such applications. Splitter plate is one of such tools that is being explored by researchers as part of passive VIV and drag reduction technique.[4, 5]

A rigid splitter plate may be used in either of the following possible configurations with circular cylinder:

- i. Fixed at the leading edge of cylinder, called frontal unilateral splitter plate,[5, 6]
- ii. Fixed at the trailing edge of cylinder, called rear/wake unilateral splitter plate,[4]
- iii. Hinged at the leading or trailing edge of cylinder, [7]
- iv. Placed at a gap from cylinder either at leading or rear end of cylinder, detached frontal and rear splitter plate[8]

A substantial magnitude of experimental and numerical work has been reported in literature on the above-mentioned configurations of circular cylinder with rigid unilateral splitter plates. In comparison a negligible amount of work is reported in literature regarding circular cylinder with attached bilateral splitter plates. In this case, two rigid splitter plates were fixed in-line with the circular cylinder both at its leading and trailing ends. The purpose of employing inline bilateral plates is to take advantage of both frontal unilateral splitter plate and rear unilateral plate. It was concluded by [6] in their research paper that when ratio of length of plate to diameter of cylinder (L/D) is set to 1, the drag reduction of 36% will be achieved at $Re\ 2.6 \times 10^4$ in case of frontal unilateral plate. It was also reported that for L/D value of 1.0, Strouhal Number (St) is 0.2005 and for L/D 2.0 Strouhal Number is 0.2238 at $Re\ 2.6 \times 10^4$. It was concluded by [9] that rear/wake unilateral splitter plate has significant impact on drag by stabilizing separation point of flow up to magnitude of 50% reduction for L/D up to 2 at $Re\ 10^4-5 \times 10^4$. [9] It was reported by [10] in their numerical that at maximum 17% reduction in the value of Strouhal Number (St) may be achieved by employing rear/wake unilateral splitter plate at 0° angle at $Re\ 100$. [10]

It is evident from the literature that rigid attached

unilateral plates have impact on C_d and St values of a circular cylinder. [11] employed attached rigid bilateral plates of dimensions: $1xD$ at the leading end and $3xD$ at the trailing edge of a circular cylinder. They concluded that the setup is successful in reducing drag for circular civil structures at Re (based on cylinder diameter) 1.66×10^5 to 8.28×10^5 ranging from sub-critical to super critical regime. [11] [12] conducted experiments on the circular cylinder with attached rigid bilateral plates of dimension: $1xD$ for front side and $1xD$ for rear side. They reported C_d becomes minimum value at L/D of 0.75 at Re 3.33×10^4 . They concluded that for circular cylinder with bilateral attached rigid splitter plates having L/D of 1, C_d is 0.5. [12]

Research papers [11, 12] have focused on circular cylinder with attached bilateral splitter plates. A gap has been observed as many engineering applications operate in a wider array of Re , especially sub-critical regime. This gap has become further vital due to the complicated behavior of fluid flow across circular cylinder at different Re . This research aims to narrow down the gap by presenting the experimental results across sub-critical regime ($300-3 \times 10^5$) in the range of Re 4.78×10^4 to 1.35×10^5 .

II. EXPERIMENTAL SETUP

The research was carried out in open circuit wind tunnel (FM-1849-28). Mesh and honeycomb structures were mounted ahead leading to turbulence intensity of $\pm 2\%$ over velocity range of 0-30m/sec. The cross section of test section is 300 mm x 300 mm and the length of the test section is 450 mm.

Test Specimen

Circular cylinder of diameter (D) 75 mm was machined to ensure perfect circular shape across the length of 225 mm with an error of less than 0.1 mm. Bilateral splitter plates were welded across the length of cylinder using arc spot welding.

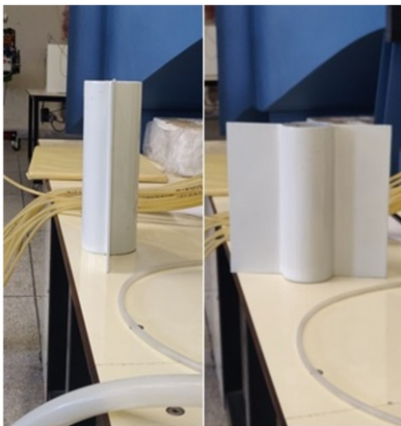


Fig. 1: Visuals of Sample of circular cylinder with attached rigid bilateral splitter plates

The plates were 75 mm wide and the thickness (t) of the plates was 4 mm to maintain $t/D \approx 0.05$ as kept by Y. Qui et. al. The extra welding was ground using electric grinder. The plates neither fluttered nor vibrated during the commencement of the experiment. The plates were installed with the accuracy of 0.5 mm from the center of circular cylinder. The visuals of the sample are given in Figure 1 and details are summarized in Figure 2.

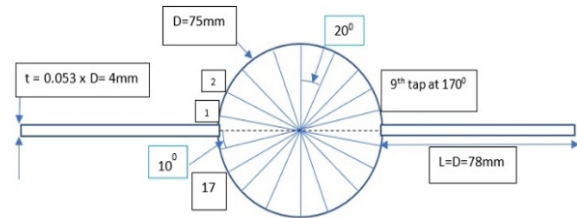


Fig. 2: Sketch of Sample of circular cylinder with attached rigid bilateral splitter plates

To remove the flaws of machining and welding, thin filler material coating was done on the surface. Automobile paint was applied to attain smooth surface finish. Smooth painted rigid endplates of 225 mm x 75 mm x 4 mm were also employed. The test specimen with end plates is shown Figure 3.

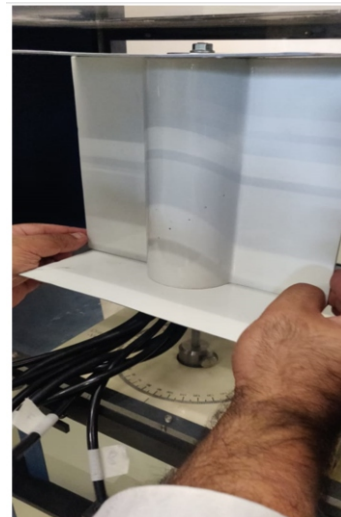


Fig. 3 Circular cylinder with attached rigid bilateral splitter plates with end plates

Pressure Taps

Pressure taps were installed on the cylinder at every 20° using cylindrical coordinate system. The taps were of stainless-steel tubes having diameter of 0.75 mm and 5 mm long. The taps directly opened in flexible plastic vacuum tubes of internal diameter of 3mm to avoid losses in 90° metallic bends. Visuals of pressure taps on sample are given in Figure 4 and positioning of pressure tap is sketched in Figure 2.



Fig. 4: Visuals of pressure taps on circular cylinder with attached rigid bilateral splitter plates

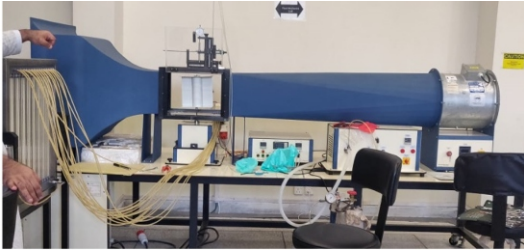


Fig. 5 Experimental set up

III. NUMERICAL SET UP

Governing equation for specific dissipation rate is as under:

$$\frac{\partial \rho \omega}{\partial t} + \text{div}(\rho \omega \mathbf{U}) = \text{div} \left[\left(\mu + \frac{\mu_t}{\sigma_{\omega,1}} \right) \text{grad}(\omega) \right] + \gamma_2 \left(2\rho S_{ij} \cdot S_{ij} - \frac{2}{3} \rho \omega \frac{\partial U_i}{\partial x_j} \delta_{ij} \right) - \beta_2 \rho \omega^2 + 2 \frac{\rho}{\sigma_{\omega,2} \omega} \frac{\partial k}{\partial x_k} \frac{\partial \omega}{\partial x_k} \quad (1)$$

Where,

$\frac{\partial \rho \omega}{\partial t}$ is rate of change of ω ,

$\rho \omega \mathbf{U}$ is transport of ω by convection,

$\left(\mu + \frac{\mu_t}{\sigma_{\omega,1}} \right) \text{grad}(\omega)$ is transport of ω by diffusion,

$\gamma_2 \left(2\rho S_{ij} \cdot S_{ij} - \frac{2}{3} \rho \omega \frac{\partial U_i}{\partial x_j} \delta_{ij} \right)$ is rate of production of ω ,

$\beta_2 \rho \omega^2$ is rate of destruction of ω ,

$2 \frac{\rho}{\sigma_{\omega,2} \omega} \frac{\partial k}{\partial x_k} \frac{\partial \omega}{\partial x_k}$ is cross diffusion term.

Specific dissipation rate is related to dissipation rate as:

$$\varepsilon = k \omega \quad (2)$$

Solver Settings & Numerical Scheme

ANSYS Fluent[®] tool has been employed for numerical methods.

Density based solver was selected to handle any variation in density of fluid for the leading side of the cylinder. Transient time is opted to invoke URANS. Implicit numerical scheme was selected to ensure

stability of solution. Roe flux-difference splitting (Roe-FDS) was used to model convective flux as there were no discontinuities/ shock waves expected in the flow. Green-Gause node based spatial discretization was selected as it ensures second order accuracy of discretization in calculating gradients from adjacent cells. Second order upwind scheme was selected for pressure and momentum equations to get higher accuracy at faces of cell. First order upwind schemes were used to discretize turbulent kinetic energy and specific dissipation rates for stable solution. Transient first order implicit formulation selected as it was more stable than second order implicit formulation.

Fluid Domain

Fluid domain was $20 \times D = 20 \times 1.6 = 32$ m in front, $50 \times D = 50 \times 1.6 = 80$ m rear and $15 \times D = 15 \times 1.6 = 24$ m on both sides from the center of circular cylinder with attached rigid bilateral plates as sketched in Fig. 6.

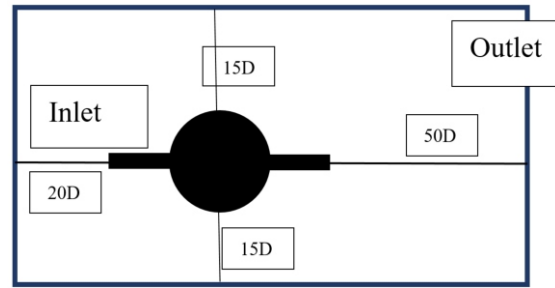


Fig. 6: Fluid domain

Meshing

Fluid domain was splatted to ensure structured quadrilateral elements of structured mesh. Boundary layer with first layer height of $2.5 \mu\text{m}$ was introduced using inflated 25 layers.

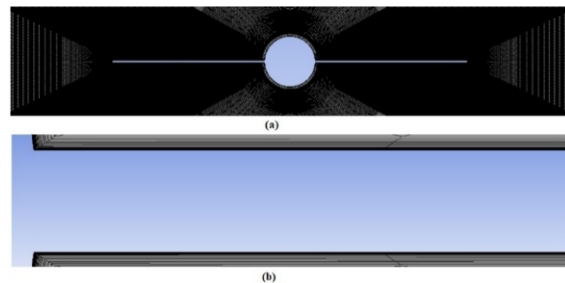


Fig. 7: Meshing for circular cylinder with attached fixed rigid bilateral plate 1xD 1xD:

(a) Close up view (b) Boundary inflation layers

Boundary Conditions

Boundary conditions employed are tabulated below:

Table 1: Boundary conditions for circular cylinder with attached rigid bilateral splitter plates

Inlet	Outlet	Cylinder Walls	Side Walls
Velocity (m/s)	0 Pa	No Slip Condition	0 Specific Shear

Table2: Values of coefficient of drag calculated from Cp values

Sr. No.	Re	Cd
1	4.78x10 ⁴	0.482
2	5.77 x10 ⁴	0.499
3	6.91 x10 ⁴	0.499
4	8.14 x10 ⁴	0.551
5	8.67 x10 ⁴	0.598
6	9.12 x10 ⁴	0.581
7	1.00 x10 ⁵	0.531
8	1.09 x10 ⁵	0.499
9	1.16x10 ⁵	0.481
10	1.21 x10 ⁵	0.455
11	1.30 x10 ⁵	0.420
12	1.35 x10 ⁵	0.409

IV. RESULTS & DISCUSSION

Co-efficient of pressure (Cp) was calculated at each pressure tap using the following equation:[11]

$$C_p = \frac{P - P_\infty}{\rho_a U^2} \quad (3)$$

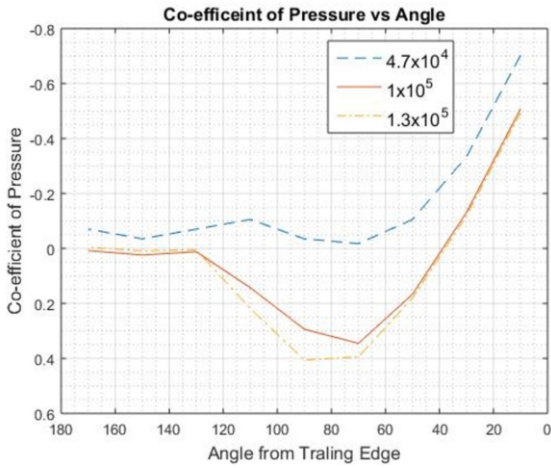


Fig. 8: Pressure Co-efficient at cylinder surface in presence of attached rigid bilateral splitter plates

Cp shows increasing trend in magnitude at higher Re, because, inertial forces at higher Re dominate viscous forces. Figure 8 peak values of Cp to occur between 70^o-90^o in contrast to that of bare cylinder that was between 70^o-80^o. This shows that bilateral splitter plates have made the pressure distribution over cylinder surface spread out. This happens to lower peak values of pressure on cylinder surface.

Table 2 presents values of Cd calculated by using equation II at Re 4.78x10⁴, 5.77 x10⁴, 6.91 x10⁴, 8.14 x10⁴, 8.67 x10⁴, 9.12 x10⁴, 1.00 x10⁵, 1.09 x10⁵, 1.21 x10⁵, 1.30 x10⁵ and 1.35 x10⁵. [11]

$$C_d = \int_0^{2\pi} C_p \cos\theta \, d\theta \quad (4)$$

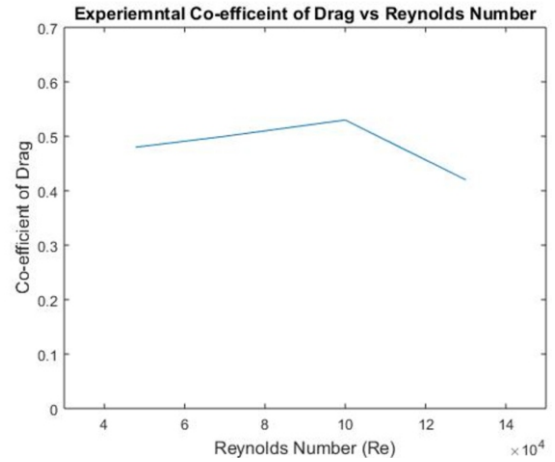


Fig. 9: Experimental coefficient of drag vs Re

Experimental results of this research in the lower range of Re were found close to the results of [12] for same geometrical configuration, thus validating the results of this research. The expected, values of Cd were higher than those of [11], because of longer length of rear plate employed by [11], and this difference confirms the validity of the research for higher values of Re.

Table 3 presents the percentage decrease in value of Cd after employing 1 x D bilateral splitter plated in sub-critical regime. It becomes clear from the table that attached rigid bilateral splitter plates of length 1xD reduce Cd substantially.

Table 3: Percentage reduction of Cd with respect to a bare cylinder

Re	Cd	$\frac{C_{dc}}{C_d}$ (Bare Cylinder)[13]	%age Reduction $\frac{C_{dc}-C_d}{C_{dc}} \times 100$
4.78×10^4	0.482	≈ 1.2	60%
5.77×10^4	0.499	≈ 1.2	58%
6.91×10^4	0.499	≈ 1.2	58%
8.14×10^4	0.551	≈ 1.2	54%
8.67×10^4	0.598	≈ 1.2	50%
9.12×10^4	0.581	≈ 1.2	52%
1.00×10^5	0.531	≈ 1.2	56%
1.09×10^5	0.499	≈ 1.2	58%
1.16×10^5	0.481	≈ 1.2	60%
1.21×10^5	0.455	≈ 1.2	62%
1.30×10^5	0.420	≈ 1.2	65%
1.35×10^5	0.409	≈ 1.2	66%

Numerical simulations for circular cylinder with attached bilateral splitter plates ($1 \times D \ 1 \times D$) have been carried out at $Re \ 4.78 \times 10^4$, 6.9×10^4 , 1×10^5 , 1.3×10^5 and 5×10^5 . Velocity contours at $Re \ 4.78 \times 10^4$ and 6.9×10^4 , are shown in Figure 10 & 11. Separation bubbles are observed to shed along rear plate till they merge to form larger bubble. Boundary layer thickness increases along frontal plate length. Velocity gradients in the layer build up at higher Re.

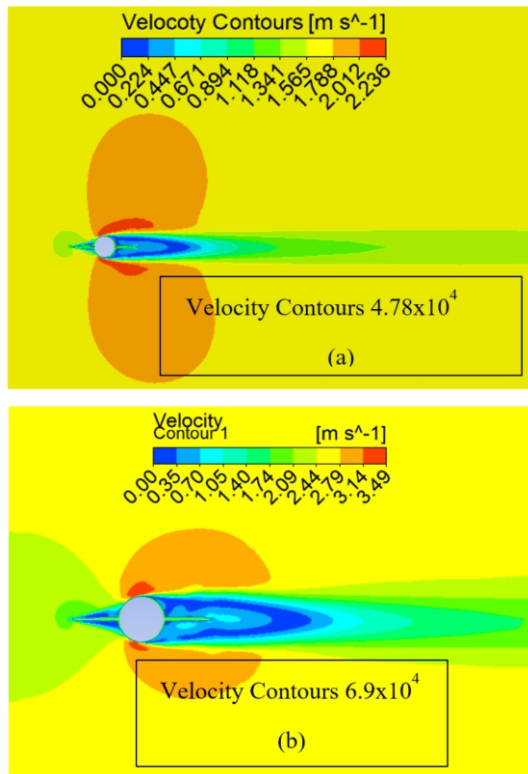


Fig. 10: Velocity contours Circular cylinder with attached bilateral splitter plates ($1 \times D \ 1 \times D$) at Re: (a) 4.78×10^4 , (b) 6.9×10^4

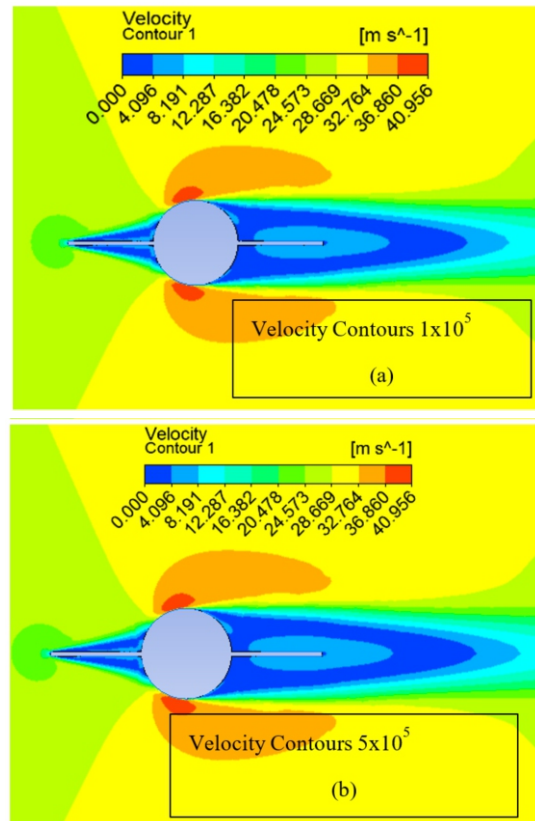


Fig. 11: Velocity contours Circular cylinder with attached bilateral splitter plates ($1 \times D \ 1 \times D$) at Re: (a) 1×10^5 , (b) 5×10^5

Experimental and numerical Cd and St at $Re \ 4.78 \times 10^4$, 6.9×10^4 , 1×10^5 , 1.3×10^5 and 5×10^5 are given in Table 4. St has decreased in comparison to a bare cylinder, however, simulations overpredict Cd as expected of 2D URANS.

Table 4: Coefficient of drag in Sub-Critical Regime for Circular cylinder with attached bilateral splitter plates ($1 \times D \ 1 \times D$)

Re	Cd (Simulation)	Cd (Experimental)	St (Simulation)
4.78×10^4	0.5	0.48	0.0018
6.90×10^4	0.54	0.499	0.002
1.00×10^4	0.56	0.53	0.003
1.30×10^5	0.45	0.42	0.07
5.00×10^5	0.44	N/A	N/A

In Figure 12 presents numerically calculated and experimentally found Cd graphically. Both are in close agreement with each other.

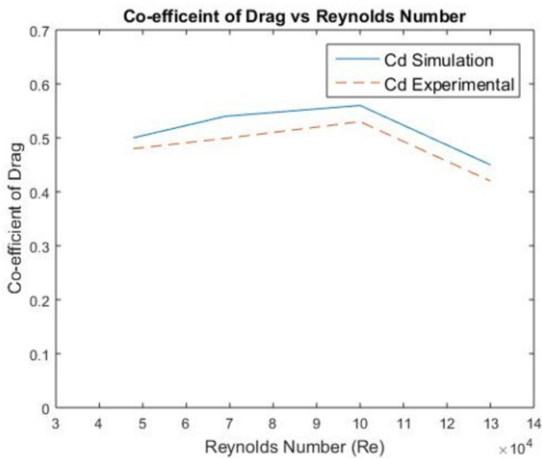


Fig. 12: Experimental and Simulation Coefficient of drag vs Reynolds Number in Sub-Critical Regime for Circular cylinder with attached bilateral splitter plates (1xD 1xD)

VI. CONCLUSION

In this research, fluid flow across circular cylinder with attached rigid bilateral splitter plates has been experimentally and numerically explored at Re 4.78×10^4 , 5.77×10^4 , 6.91×10^4 , 8.14×10^4 , 8.67×10^4 , 9.12×10^4 , 1.00×10^5 , 1.09×10^5 , 1.21×10^5 , 1.30×10^5 and 1.35×10^5 in sub-critical regime. Experiments show that bilateral splitter plates decrease Cd up to 66% for simple circular cylinder with attached bilateral splitter plates. This is because, gradients of pressure and velocity of a bare cylinder were reduced by bilateral splitter plates.

Attached rigid bilateral splitter plates reduce St to values of 0.0018, 0.002, 0.002 and 0.07 at Re 4.78×10^4 , 6.91×10^4 , 1.00×10^5 and 1.30×10^5 , respectively, that are negligible. This is so because velocity gradients of vortices are reduced because of presence of boundary layers of attached bilateral splitter plates overcomes adverse variations in pressure behind the cylinder.

In light of the findings of this research, it is concluded that circular cylinder with attached bilateral splitter plates has the ability to reduce drag and vortex induced vibration as observed in the landing gear of an aero plane. Hence circular cylinder with attached bilateral splitter plates can be used for landing gear strut of an aero plane to reduce drag as well as vortex induced vibration.

REFERENCES

[1] L. Pagnini, G. Piccardo, and G. Solari, "VIV regimes and simplified solutions by the spectral model description," *Journal of Wind Engineering and Industrial Aerodynamics*, vol. 198, p. 104100, 2020.
[2] R. Zhou, Y. Ge, Y. Yang, Y. Du, and L. Zhang,

"Aerodynamic performance evaluation of different cable-stayed bridges with composite decks," *Steel and Composite Structures*, vol. 34, pp. 699-713, 2020.
[3] M. I. Khan and S. A. Masood, "A Numerical Investigation of Vortex Shedding and Flow around a Smooth Circular Cylinder in Upper Transition Regime by Using URANS," *Technical Journal*, vol. 25, pp. 15-21, 2020.
[4] K. Kwon and H. Choi, "Control of laminar vortex shedding behind a circular cylinder using splitter plates," *Physics of Fluids*, vol. 8, pp. 479-486, 1996.
[5] B. An, J. Bergadà, F. Mellibovsky, W. Sang, and C. Xi, "Numerical investigation on the flow around a square cylinder with an upstream splitter plate at low Reynolds numbers," *Meccanica*, pp. 1-23, 2020.
[6] D. Gao, G. Chen, Y. Huang, W. Chen, and H. Li, "Flow characteristics of a fixed circular cylinder with an upstream splitter plate: on the plate-length sensitivity," *Experimental Thermal and Fluid Science*, p. 110135, 2020.
[7] S. Cheng, Y. Jin, and L. P. Chamorro, "On the multiscale oscillations of a hinged plate under stratified coherent motions," *Journal of Fluids and Structures*, vol. 94, p. 102944, 2020.
[8] H. Zhu, G. Li, and J. Wang, "Flow-induced vibration of a circular cylinder with splitter plates placed upstream and downstream individually and simultaneously," *Applied Ocean Research*, vol. 97, p. 102084, 2020.
[9] C. Apelt, G. West, and A. A. Szewczyk, "The effects of wake splitter plates on the flow past a circular cylinder in the range $10^4 < R < 5 \times 10^4$," *Journal of Fluid Mechanics*, vol. 61, pp. 187-198, 1973.
[10] R. Abdi, N. Rezazadeh, and M. Abdi, "Reduction of fluid forces and vortex shedding frequency of a circular cylinder using rigid splitter plates," *European Journal of Computational Mechanics*, vol. 26, pp. 225-244, 2017.
[11] Y. Qiu, Y. Sun, Y. Wu, and Y. Tamura, "Effects of splitter plates and Reynolds number on the aerodynamic loads acting on a circular cylinder," *Journal of Wind Engineering and Industrial Aerodynamics*, vol. 127, pp. 40-50, 2014.
[12] D. Gao, Y. Huang, W.-L. Chen, G. Chen, and H. Li, "Control of circular cylinder flow via bilateral splitter plates," *Physics of Fluids*, vol. 31, p. 057105, 2019.
[13] C. Scruton and E. Rogers, "Steady and unsteady wind loading of buildings and structures," *Philosophical Transactions of the Royal Society of London. Series A, Mathematical and Physical Sciences*, vol. 269, pp. 353-383, 1971.